Biogeosciences Discuss., doi:10.5194/bg-2016-413, 2016
Manuscript under review for journal Biogeosciences
Published: 20 October 2016

Biogeosciences Discussions Open Access EGU

The Oxic Degradation of Sedimentary Organic Matter 1.4 Ga Constrains Atmospheric Oxygen Levels

Shuichang Zhang[1], Xiaomei Wang[1], Huajian Wang[1], Emma U. Hammarlund[2], Jin Su[1], Yu Wang[1], Donald E. Canfield[2]

[1]Key Laboratory of Petroleum Geochemistry, Research Institute of Petroleum Exploration and Development, China National Petroleum Corporation, Beijing 100083, China

[2]Department of Biology and Nordic Center for Earth Evolution (NordCEE), University of Southern Denmark, Campusvej 55, 5230 Odense M, Denmark

Corresponding to Shuichang Zhang (sczhang@petrochina.com.cn)

Abstract. We studied sediments from the ca. 1400 million-year-old Xiamaling Formation from the northern China Block. The upper unit of this formation (unit 1) deposited mostly below storm wave base and contains alternating black and green-gray shales with very different geochemical characteristics. The black shales are enriched in redox sensitive trace metals, have high concentrations of total organic carbon (TOC), high hydrogen index (HI) and iron speciation indicating deposition under anoxic, mostly euxinic, conditions. In contrast, the green-grey shales show no trace metal enrichments, low TOC, low HI and iron speciation consistent with an oxygenated depositional setting. Altogether, unit 1 displays alternations between oxic and anoxic depositional environments, and differences in carbon preservation consistent with observations from the modern ocean. We combined our TOC and HI index results to calculate the differences in carbon mineralization between the oxygenated and anoxic depositional environments. Through comparisons of these results with modern sedimentary environments, and by use of a simple diagenetic model, we conclude that carbon mineralization under oxygenated conditions at Xiamaling required a minimum of 4% to 8% of present-day oxygen levels (PAL). These oxygen levels are higher than estimates based on chromium isotopes and, furthermore, were likely sufficient for early animal respiration. Therefore, our results reinforce the idea that the environment contained enough oxygen for animals long before their evolution.

Keywords

Atmospheric oxygen; Mesoproterozoic; hydrogen index; carbon preservation; oxic respiration; anoxic; animal evolution; marine sediment

Biogeosciences Discuss., doi:10.5194/bg-2016-413, 2016
Manuscript under review for journal Biogeosciences
Published: 20 October 2016

1 Introduction

The Mesoproterozoic Era (1600 to 1000 million years ago, Ma) was a time of profound biological transition. It witnessed the emergence of nascent eukaryote ecosystems, and more generally, it linked the dominantly prokaryote world of the Paleoproterozoic Era (2500 to 1600 Ma), and before, to the Neoproterozoic Era (1000 to 541 Ma), where eukaryotes greatly diverged and where animals first evolved (Butterfield, 2015; Knoll, 2014). In a widely held view, limited oxygen availability may have restricted the evolution and diversification of eukaryote clades, including animals, until a permissive environment emerged with a rise in oxygen levels in the late Neoproterozoic Eon (Berkner and Marshall, 1965; Knoll, 2011, 2014; Nursall, 1959).

Unfortunately, there are few constraints on oxygen levels during the Mesoproterozoic Era. The original idea that Mesoproterozoic oceans were largely anoxic below the surface mixed zone generated maximum oxygen concentrations in the range of 40% of present atmospheric levels (PAL) (Canfield, 1998). Subsequently, low concentrations of redox-sensitive trace metals like U and Mo in black shales have reinforced the idea of wide-spread Mesoproterozoic ocean anoxia and lower levels of atmospheric oxygen (Partin et al., 2013; Scott et al., 2008). Recently, the lack of observable fractionation in chromium-associated with Fe-enriched marine sediments has suggested a lack of oxidative weathering of chromium minerals on land, and subsequently, atmospheric oxygen levels of $\leq 0.1\%$ PAL (Planavsky et al., 2014), an idea reinforced by low Cr isotope fractionations preserved in Mesoproterozoic shales (Cole et al., 2016b). In contrast, sediments from unit 3 of the Xiamaling Formation demonstrate trace metal and biomarker signatures consistent with deposition in oxygenated waters below an ancient oxygen-minimum zone (OMZ) (Zhang et al., 2016). A simple ocean-carbon model demonstrated that $\geq 4\%$ PAL was needed to have oxygenated these deep marine waters (Zhang et al., 2016). Thus, available constraints on Mesoproterozoic levels of atmospheric oxygen are contradictory, and clearly, other lines of evidence are required to constrain the evolution of Mesoproterozoic atmospheric oxygen and its role in biological evolution. Here, we report evidence from unit 1 of the Xiamaling Formation for sediment oxygenation and oxic organic matter mineralization. These observations combine with a simple diagenetic model to constrain atmospheric oxygen to a minimum of 4 to 8 % PAL.

2 Study site and methods

Biogeosciences Discuss., doi:10.5194/bg-2016-413, 2016
Manuscript under review for journal Biogeosciences
Published: 20 October 2016

2.1 Study site

We explored rocks from the Xiamaling Formation of the North China Block. The Xiamaling Formation is part of Paleoproterozoic to Mid-Mesoproterozoic sedimentary sequence, depositing onto Paleoproterozoic crystalline rocks that were likely formed during the breakup of supercontinent Columbia (Meng et al., 2011). The sedimentary sequence begins as an opening rift basin that developed into a passive margin and eventually a back-arc setting (Meng et al., 2011; Qu et al., 2014). The Xiamaling Formation itself contains relatively few volcanoclastic layers, and was first intruded by diabase sills at 1323 ± 21 Ma (Li et al., 2009). These intrusive sills are taken to indicate back-arc development, but some 60 to 70 million years after sediment deposition dated with high-precision thermal ionization mass spectrometry (TIMS) at 1384.4 ± 1.4 Ma for a tuff layer located at 210 m depth in the stratigraphy, and 1392.2 ± 1.0 Ma for a bentonite layer 52 m below the tuff level (Zhang et al., 2015). Thus, the Xiamaling Formation likely deposited in a passive-margin setting like the sediments depositing just before (Meng et al., 2011; Qu et al., 2014). Overall, the Xiamaling Formation has a total thickness of about 450 m, and is composed of highly-laminated sediments deposited, mostly, in deeper quiet waters below storm wave base (>100 m) through most of its history (Zhang et al., 2015). The sediments are also of exceptionally low thermal maturity, likely never heated to greater than 90^{o}C (Zhang et al., 2015).

The Xiamaling Formation deposited in a tropical to sub-tropical setting between 10^{o}N and 30^{o}N latitude (Zhang et al., 2012), and the patterns of sediment lamination and chemistry are consistent with the influence of climate forcing on sedimentation dynamics (Zhang et al., 2015). We focus here on the upper 45 meters of the Xiamaling Formation, as contained within unit 1. This part of unit 1 is composed of centimeter-scale alternations between high-TOC black shales and low-TOC green-gray shales (Zhang et al., 2015). Previous work placed this unit in the downwelling limb of an ancient Hadley Cell where fluctuations in sediment chemistry resulted from periodic changes in Hadley Cell placement and the location of the Intertropical Convergence Zone (ITCZ) as these influenced patterns of trade wind intensity and ocean circulation (Zhang et al., 2015).

A deep-water setting is indicated through most of the unit 1, but at about 15 m depth, there appear occasional strata with hummocky-cross bedding indicating the influence of storm

Biogeosciences Discuss., doi:10.5194/bg-2016-413, 2016
Manuscript under review for journal Biogeosciences
Published: 20 October 2016

waves on deposition. From here and upwards, the sediments deposited at or above storm wave base, which can range in depth from about 50 to 200 meters (Immenhauser, 2009). Thus, overall, unit 1 likely deposited in waters in the depth range of 100 ± 50 meters, with deeper waters towards the bottom of the unit and shallower waters towards the top.

2.2 Sample collection and analytical methods

Both outcrop and core samples from the Xiamaling Formation were used in this study. Outcrop samples were collected at ~0.5m intervals along road cuts within 2 to 4 y after they were made.

The different rock types were easy to discriminate in outcrop, and all samples were collected after removal of the weathered outer layer (see further(Zhang et al., 2015)). Core samples were collected using a diamond drill lubricated with fresh water to minimize contamination from drilling fluids (see further (Zhang et al., 2016)). Core depths were correlated to outcrop height based on reconstructions from drilling depth and angle and cross calibration of geochemical parameters. For geochemical analyses, all samples were rinsed with purified water, dried, and then crushed to fine powder (less than 74 μm) using a stainless steel puck mill, which was cleaned between samples by grinding with baked quartz sand multiple times. All of the geochemical data were obtained from the homogeneous powder.

Trace metal concentrations were measured by ICP-MS following the methods outlined in (Zhang et al., 2015). Accuracy was tested with the shale standard (GBW 03014) that was measured along with the samples and determined to be within 3.0 % for V, 11% for Mo and 17% for U. The major elements were measured with X-ray fluorescence. Accuracy was tested with the whole-rock standard materials (GBW 07109-07112), and the relative standard deviation of major element concentrations was < 1%.

The HI expresses the amount of bound hydrocarbon-like compounds released during sample pyrolysis, ratioed against the total amount of organic carbon (TOC) in the sample (Espitalie et al., 1977). HI is defined as S_2*100/TOC (Espitalié, 1986; Tissot and Welte, 1984){Espitalié, 1986 #1109;Tissot, 1984 #1469}, where S_2 is the longer-chained, non-volatile hydrocarbons cracked and liberated during heating pyrolysis. Pyrolysis was accomplished by programmed heating of samples in Rock-Eval 6 (Vinci Techologies, France), operating with software ROCKINT for data interpretation, with a nitrogen (N_2) atmosphere. The initial and final

Biogeosciences Discuss., doi:10.5194/bg-2016-413, 2016
Manuscript under review for journal Biogeosciences
Published: 20 October 2016

pyrolysis temperatures were 300 ℃ and 650 ℃, respectively, and the programmed heating rate was 25 ℃/min. The instrument was calibrated using standard material [GBW (E) 070064~070066].

The measurement of total organic carbon (TOC) on outcrop samples was performed at the Key Laboratory of Petroleum Geochemistry in China. All samples were powdered and de-carbonated (1M HCl for 2 h), and subsequently dried. TOC concentrations were measured with a LECO CS-230HC carbon-sulfur analyzer. TOC on core samples was determined after de-carbonation (same as for outcrop samples) at the Nordic Center for Earth Evolution (NordCEE), University of Southern Denmark, on a Thermo Analytical element analyzer Flash EA 2000. Analytical uncertainties for all TOC analyses were less than 5% based on the concentrations of known standard materials (n=5 for analyses in China and n=11 for analyses in Denmark).

Isolation of kerogen involves successive removal of soluble organic matter (bitumen), mineral matter, and water from the shale, such that predominantly kerogen remains. The sediment powders were extracted for 72 h using a Soxhlet apparatus (9:1 v/v DCM/MeOH) to remove soluble bitumen. Minerals in the sediments were then removed with the following procedure: 1) carbonates were dissolved by reacting with 6 mol l^{-1} HCl at 60 to 70 ℃ for 1 to 2 h, 2) silicates were dissolved by reacting with a mixture of 40% HF and 6 M HCl (3:2 v/v) at 60 ~ 70 ℃ for 2 h, 3) newly formed fluorides were removed with 3% HNO_3. After each step, the samples were flushed with deionized water to remove soluble material. The kerogen was finally obtained as a coarse malleable mass after drying overnight at 90 ℃.

The isotopic composition ($\delta^{13}C_{org}$) of dry kerogen was measured with a Delta V Advantage mass spectrometer (Thermo Scientific Co. Ltd.) after the carbon was first combusted to carbon dioxide using a Flash EA 1112 HT. The mass spectrometer was standardized with NBS-18 ($\delta^{13}C$ = -5.014‰) and GBW04405 ($\delta^{13}C$ = 0.57‰) standards with a relative standard deviation of 0.2‰ based on replicate analyses of the standards (n=5). Isotopic compositions are reported relative to the Pee Dee Belemnite (PDB).

Iron speciation was performed on powders of samples collected from fresh core material. The analytical method followed that of (Poulton and Canfield, 2005). In the Fe speciation technique, four different pools of highly iron (FeHR) are evaluated. These are: carbonate

Biogeosciences Discuss., doi:10.5194/bg-2016-413, 2016
Manuscript under review for journal Biogeosciences
Published: 20 October 2016

associated iron (FeCARB; siderite or ankerite), ferric oxide and ferric oxyhydroxide minerals (FeOX; ferrihydrite, lepidocrocite, goethite, hematite), magnetite (FeMAG) and sulfidized iron, mainly pyrite (FePY). The concentrations of the non-sulfidized iron pools were quantified by atomic adsorption spectroscopy (AAS), and the analytical error for each iron extraction was less than 5% (as monitored through comparisons with the internally calibrated extractions of NRC PACS-2 and PACS-3 sediment standards, n=5 per set of outcrop and core samples). Pyrite sulfur was extracted by chromium digestion, trapped as Ag_2S, and its concentration determined gravimetrically (Canfield et al., 1986; Zhabina and Volkov, 1978). Replicate extractions of the sediment standard NRC PACS-2 indicate an analytical error for evaluating pyrite iron contents of less than 9 % (n=6 per set core sample set). The sum of the four pools of reactive iron gives the total concentration of the highly reactive iron (FeHR). The Fe (HR) is normalized to the total concentration of Fe in the sample (FeT), yielding the ratio FeHR/FeT.

Total iron concentrations were obtained through X-ray fluorescence (XRF) analysis at the PetroChina laboratory (China), handheld XRF (HHXRF) analysis at the University of Southern Denmark (see methods outlined in (Zhang et al., 2016)), as well as through wet extractions (boiling HCl) at SDU in Denmark. In determining the total Fe through XRF, the relative standard deviation (SD) was less than 1.0% and the accuracy was 0.2 % (n=5) against shale standard material (GBW 03014). Iron determinations through both HHXRF and the wet extractions were calibrated against the PACS-2 standard and the error determined to be less than 5% (n=33) in the case of HHXRF and less than 8% in the case of wet extractions (n=22). Total Fe extracted through the different methods XRF, HHXRF and HCl were compared in split samples (n=24) from the Xiamaling unit 3. The correlations of FeT in these samples of data obtained with XRF and HHXRF (slope=0.9) and of data obtained with XRF and HCl (slope=1.0) both have an r^2 value > 0.99 respectively.

The ratio of highly reactive iron over total iron (FeHR/FeT) rarely exceeds 0.38 during oxic deposition, as observed in modern sediments (Raiswell and Canfield, 1998). FeHR/FeT values above 0.38, in contrast, are often found in sediments below anoxic water columns, both in modern and ancient depositional settings (Poulton and Raiswell, 2002; Raiswell and Canfield, 1998). Still, the pool of reactive iron can be influenced by rapid sedimentation (Poulton et al., 2004; Raiswell and Canfield, 1998) and diagenesis (Poulton and Canfield, 2011) and references

Biogeosciences Discuss., doi:10.5194/bg-2016-413, 2016
Manuscript under review for journal Biogeosciences
Published: 20 October 2016

therein), yielding lower FeHR/FeT values. Therefore, while FeHR/FeT values above 0.38 can be taken to indicate anoxic water column conditions, values below 0.38 do not necessarily represent oxic deposition and other geochemical indicators are best applied to evaluate oxic deposition conditions as explored in more detail below.

3 Results

The results for TOC concentration, $\delta^{13}C$, HI and our trace metal analyses are shown in Table S1, while Fe speciation results are shown in Table S2. Many geochemical patterns correlate with rock type and TOC content as seen in Figure 1. Compared to the green-gray shales, the black shales show elevated TOC and HI and also elevated concentrations of Mo, V and U, as expressed through ratios with Al. Indeed, the green-grey shales show Mo/Al and V/Al ratios just at the crustal average value, and the U/Al ratio is very close to the crustal average value. In the black shales, the ratio of Fe/Al tends towards higher values, particularly below 15 m in the stratigraphy (Figure 1). Iron speciation shows that elevated ratios of FeHR/FeT are generally associated with samples containing high-TOC, and trace metal enrichment, as shown through the V/Al ratio (Figure 2).

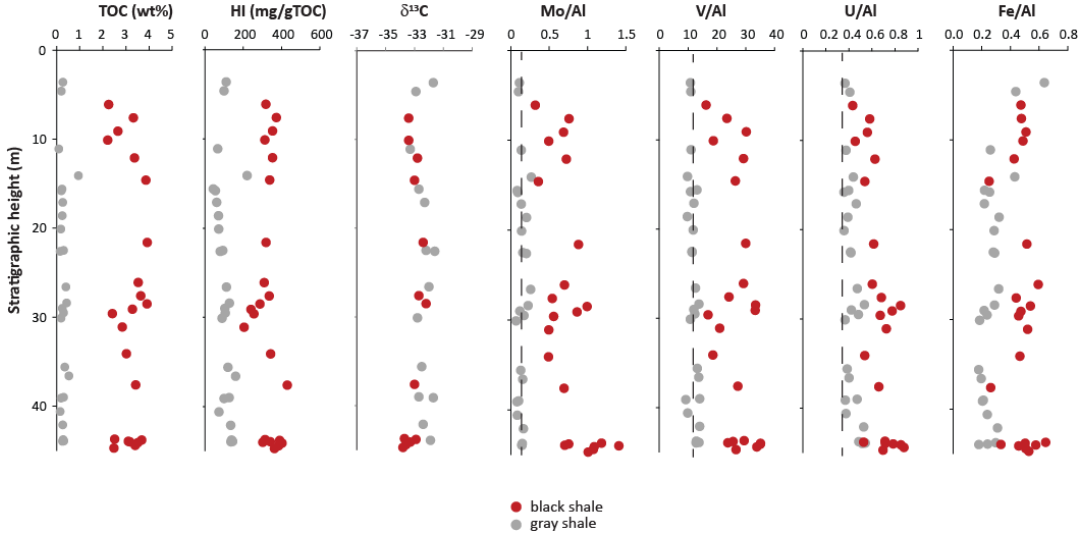

Figure 1. Total organic carbon (TOC), HI, $\delta^{13}C$ (relative to PDB) and metal data (Mo/Al, V/Al and U/Al, Fe/Al; where the dashed line represents upper crust values from (Rudnick, 2004)), for unit 1 of the Xiamaling Formation.

Biogeosciences Discuss., doi:10.5194/bg-2016-413, 2016
Manuscript under review for journal Biogeosciences
Published: 20 October 2016

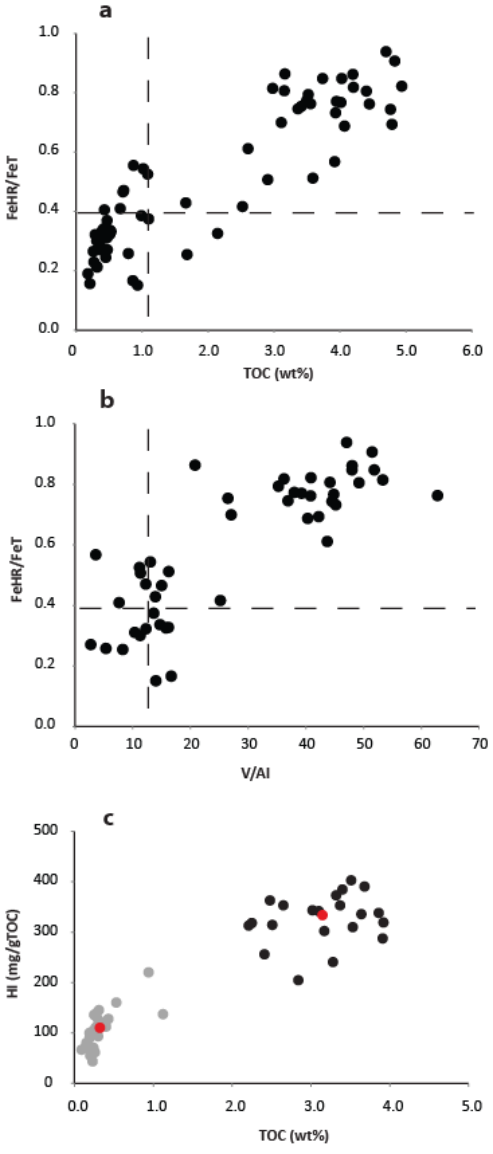

Figure 2. a) TOC vs the ratio of highly reactive to total iron (FeHR/FeT) from fresh core material in Unit 1 of the Xiamaling Formation. The horizontal dashed line represents a FeHR/FeT of 0.38, while the vertical dashed line indicates a TOC of 1 wt%. The green-gray shales are predominantly represented at TOC < 1 wt% and the black shales with TOC > 1 wt% (see Figure 1). b) V/Al vs FeHR/FeT, with the horizontal line as in a) and the vertical line the V/Al crustal average (Rudnick, 2004). c) TOC vs HI for outcrop material, with black and green-gray shales separately indicated. The red dots mark the averages for the black and green-gray shale groups.

Biogeosciences Discuss., doi:10.5194/bg-2016-413, 2016
Manuscript under review for journal Biogeosciences
Published: 20 October 2016

4 Discussion

4.1 Organic carbon preservation and water-column chemistry

We begin by considering the strong correlation between HI and TOC in unit 1 sediments of the Xiamaling Formation (Figure 1, 3). Such a correlation is also seen in sediments deposited during the Phanerozoic Eon, where HI has often been linked with the degree organic carbon preservation. In general, a higher HI is associated with more H-rich aliphatic organic matter and better organic matter preservation, while low HI is associated with poorer organic matter preservation (Espitalie et al., 1977; Tissot and Welte, 1984). Terrestrially derived lignin- and cellulose-rich organic matter (with a low HI) from vascular land plants can also contribute to low-HI values in the sediment (Espitalie et al., 1977; Tissot and Welte, 1984). This, however, is not a consideration for Mesoproterozoic-aged sediments that deposited well before land-plant evolution.

From Phanerozoic-aged examples, organic carbon preservation, as it drove correlations between TOC-HI to those for unit 1 of the Xiamaling Formation, have been ascribed to the presence or absence of oxygen during sediment diagenesis. Thus, in one example, TOC-rich, laminated to micro-burrowed shales from the Cretaceous Greenland Formation from the western interior of North America deposited with high HI, whereas moderately-to-highly bioturbated low-TOC shales deposited with low HI (Pratt, 1984). Palynological and organic geochemical analyses revealed a limited contribution of terrestrial organic matter to all sediments, and differences in HI were attributed to the influence of oxygen on organic carbon preservation. In particular, oxygen was much more available to the bioturbated sediments compared to the laminated and micro-burrowed sediments, and more oxygen availability resulted in more extensive organic matter decomposition (Pratt, 1984), yielding lower TOC and lower HI values. In another example, careful palynological and organic-geochemical analyses from the Upper Jurassic Kashpir shales of the Volga Basin, Russia, revealed that TOC-poor low-HI sediments were most likely associated with intensive oxic organic matter decomposition, whereas TOC-rich high-HI sediments were likely deposited in a continuously anoxic environment (Riboulleau et al., 2003).

Biogeosciences Discuss., doi:10.5194/bg-2016-413, 2016
Manuscript under review for journal Biogeosciences
Published: 20 October 2016

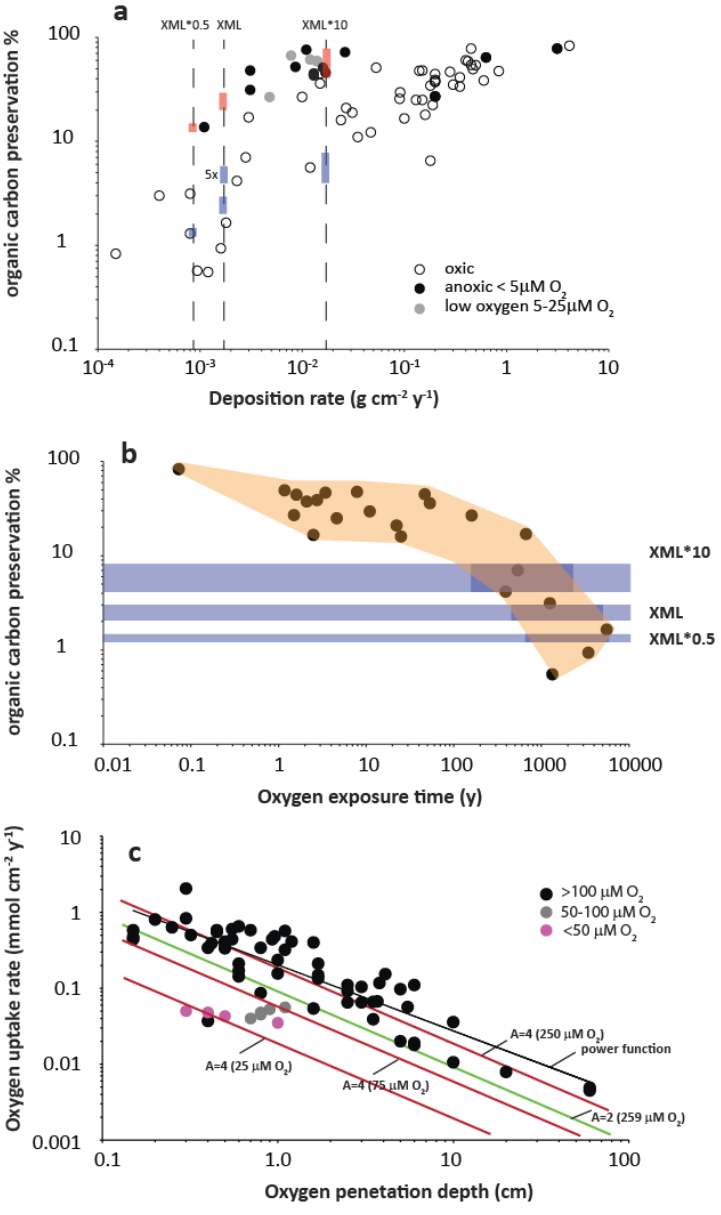

235 Figure 3. a) Preservation of organic carbon in modern marine sediments calculated as % of carbon buried in a sediment compared to the % deposited to the sediment surface. Redrafted from (Canfield, 1994).The vertical lines represent the different modelled sedimentation rates. The upper red rectangles highlight the carbon preservation for the anoxic environments in the compilation, while the lower blue rectangles are 10 times less than this, representing the estimated range of carbon preservation in Xiamaling oxic sediments. For the XML
240 sedimentation rate a blue rectangle at 5 times less carbon preservation is also shown, b) Oxygen exposure time

Biogeosciences Discuss., doi:10.5194/bg-2016-413, 2016
Manuscript under review for journal Biogeosciences
Published: 20 October 2016

versus organic carbon preservation in marine sediments. The horizontal blue boxes reflect the range of oxic sediment carbon preservation at the different sedimentation rates from a), while the dark blue fields outline the range of associated oxygen exposure times, c) oxygen penetration depth versus oxygen uptake rate from modern marine sediments with variable bottom-water oxygen concentrations. Data is from Table S4. Black line indicates the best power-function fit to the data. Red lines indicate fits from Eq. 4 to the data at different bottom water oxygen concentrations and A=4. Green line represents model fit from Eq. 4 with A=2 and 250 μM O_2.

These Phanerozoic relationships between oxygen availability and organic carbon preservation are completely consistent with both experimental observations and observations from modern marine sediments. Thus, from experiments on aged algae that was pre-decomposed for 40 days (to about one half of its initial biomass and thus representing the type of "aged" organic matter that deposits onto shelf sediments), organic matter in the presence of oxygen decomposed at rates 5 to 10 times greater compared to organic matter decomposing anaerobically (Kristensen and Holmer, 2001). These experiments were not run until labile organic matter was exhausted, but the results strongly indicate enhanced preservation of organic matter under anoxic conditions compared to preservation in the presence of oxygen. These experimental results reinforce observations from modern marine sediments (Canfield, 1994; Hartnett et al., 1998), where at the same rate of sedimentation (and for sedimentation rates <0.1 g cm^{-2} y^{-1}), sediments depositing in anoxic and low-oxygen environments preserve considerably more organic carbon compared to sediments depositing in oxygenated environments (Figure 3a) (Canfield, 1994). Here, carbon preservation (%) is defined as:

$$\%C_{pres} = 100*C_{bur}/C_{dep} = 100*C_{bur}/(C_{bur} + C_{resp}) \quad (1)$$

Where $\%C_{pres}$ is the percent of organic matter falling onto the sediment that is buried and preserved, C_{bur} is the burial flux of organic carbon, and C_{dep} is the flux of organic carbon depositing onto the sediment surface. For practical reasons, C_{dep} is usually determined as sum of the organic carbon burial flux and the rate of organic carbon respiration (C_{resp}) (Canfield, 1994, 1989).

Thus, the presence or absence of oxygen significantly influences the preservation of organic matter in sediments. Unfortunately, the relationship between organic matter preservation and HI has not been explored in modern sediments. However, for the oxygen-minimum zone

Biogeosciences Discuss., doi:10.5194/bg-2016-413, 2016
Manuscript under review for journal Biogeosciences
Published: 20 October 2016

(OMZ) of the Peruvian margin, sediment HI generally correlates with TOC, and when TOC >10 wt% in the anoxic portion of the OMZ, HI is high and in the range of 400 mg HC/gTOC. In contrast, for sediments depositing in deeper, oxygenated, waters, HI is much lower, in the range of 50 mg HC/gTOC when TOC is around 1 wt% (Arthur and Dean, 1998). Trends between HI and oxygenation, though, are somewhat blurred by sediment re-suspension and cross-shelf transport as well as particle sorting (Arthur and Dean, 1998). Such physical processes have also influenced the distribution of HI in sediments of the eastern Arabian Sea (Calvert et al., 1995; Cowie, 2005).

Returning to the Xiamaling Formation, as mentioned above, it deposited well before the evolution of terrestrial land plants, and the green-gray and black shales share similar organic matter $\delta^{13}C$ values (Figure 1) consistent with a similar source of organic carbon to each sediment type. High degrees of thermal maturity can reduce the HI (Espitalie et al., 1977; Tissot and Welte, 1984), but unit 1 sediments have all experienced the same thermal history, so this cannot account for differences in the HI between the different sediment types. We conclude, therefore, that the patterns of HI in unit 1 Xiamaling sediments indicate enhanced organic matter preservation in the high-TOC black shales compared to the low-TOC green-gray shales. Also, and by analogy with modern and ancient sedimentary environments, patterns of TOC and HI in Xiamaling unit 1 are best understood in terms of differences in carbon preservation as driven by the presence or absence of oxygen during sediment organic matter mineralization. In this view, fluctuations between TOC-rich black shales and TOC-poor shale resulted from fluctuations between anoxic and oxic depositional conditions.

This interpretation of fluctuating bottom water chemical conditions is consistent with trace metal dynamics and iron-speciation results. Thus, the redox-sensitive trace metals V, Mo and U are enriched in the black shales (Figure 1), and such enrichments are typical for deposition under anoxic water-column conditions (Brumsack, 2006). Furthermore, black shales are enriched in Fe, as expressed through the Fe/Al ratio (Figure 1), and such enrichment would indicate the enhanced deposition of Fe under anoxic bottom water conditions (Lyons and Severmann, 2006). We also see Fe enrichments from our sequential Fe extraction of the core samples. Thus, from these results, the ratio FeHR/FeT exceeds 0.38 for sediments with TOC exceeding 1 to 2 wt% (Figure 2a); these TOC levels are comparable to those for black shales from outcrop material

Biogeosciences Discuss., doi:10.5194/bg-2016-413, 2016
Manuscript under review for journal Biogeosciences
Published: 20 October 2016

(Figure 1). As mentioned above, when FeHR/FeT exceeds 0.38 this is generally taken to indicate sediment deposition under bottom-water anoxia (Raiswell and Canfield, 2012, 1998). Furthermore, samples deposited with elevated FeHR/FeT are also generally associated with elevated V/Al as would be expected for anoxic depositional environments (Figure 2b) (Lyons and Severmann, 2006; Raiswell and Canfield, 2012).

In contrast, the low-TOC green-gray shales from outcrop show either low or no enrichments in U, Mo and V (Figure 1). They also have low values of Fe/Al and, from the Fe extraction results of core material, low TOC also have low ratios of FeHR/FeT below the anoxic threshold (Figure 2). Taken together, these geochemical indicators are consistent with an oxic depositional environment for the green-gray shales, and overall support depositional environment interpretations from TOC and HI systematics.

4.2 Constraining oxygen levels

As discussed above, our geochemical results indicate considerable amounts of oxic organic matter decomposition during the deposition of the green-grey shale units of unit 1. High amounts of oxic degradation are obvious from differences in the HI between the green-gray shales and the black shales, and also in TOC concentration, where the average TOC for the black shales is 3.2 wt% and 0.33 wt% for the green-gray shales, nearly 10 times reduced (Figure 2c). In what follows, we use observations from modern environment to convert these trends in carbon preservation to organic matter mineralization rates, and from here, to the minimum levels of atmospheric oxygen needed to drive these rates of mineralization.

To begin, we recognize that organic carbon mineralization occurs both in sediments and in the water column, and therefore, we must consider how both environments contribute to organic carbon preservation. As our model is based on differences in organic carbon preservation between sediments deposited in oxic and anoxic settings, we consider first the potential role of water column mineralization in generating these differences. In one of the few studies to address this issue directly, (Keil et al., 2015) explored with sediment traps the composition of particles settling through waters of the Arabian Sea. In two stations, the water column was nitrite-containing and completely anoxic between 130-150 meters to > 500 meters water depth, while at a third site, oxygen began to accumulate at about 200 meters water depth, below a narrow anoxic

Biogeosciences Discuss., doi:10.5194/bg-2016-413, 2016
Manuscript under review for journal Biogeosciences
Published: 20 October 2016

zone. By 500 meters depth, TOC averaged about 11 wt% for particles settling through oxygenated waters and 15 wt% for particles settling through anoxic OMZ waters (Keil et al., 2015). Thus, in the Arabian Sea, there is a relatively small difference (27%) in the carbon content of particles settling through oxic and anoxic waters to 500 meters depth. We would expect this difference to be even smaller for particles settling to depths of 50 to 200 meters, representing the likely water depth range for the parts of the Xiamaling Formation unit 1 we are exploring. The Arabian Sea results also reinforce a general observation that particles settling though the upper layer of oxygenated marine waters (100s of meters) are quite TOC-rich, with values much higher (typically 3 to 15 wt%) (Armstrong et al., 2002; Honjo et al., 1982) than those observed in the green-gray shales of unit 1. Thus, the differences in the TOC content between the green-gray and black shales in unit 1 were most likely driven by differences in sediment organic carbon preservation, as determined by the presence or absence of bottom water oxygen.

We will now draw from modern observations and develop a simple sediment diagenetic model to constrain the oxygen levels required to account for the patterns of carbon preservation in Xiamaling unit 1. First, however, we note that even though the TOC content of particles settling through the oxic and anoxic water columns of Xiamaling unit 1 was likely similar, some 20% to 60 % of the settling organic matter likely mineralized as particles settled from the base of the upper mixed layer to the sediment surface at some 50 to 200 meters water depth (e.g. (Keil et al., 2015; Lamborg et al., 2008; Marsay et al., 2015; Martin et al., 1987)). This organic matter mineralization amounts to an oxygen sink and a reduction in water column oxygen levels, that is not included in our model. To include this oxygen sink would raise our minimum oxygen estimates by the magnitude of the sink. Thus, ignoring this oxygen sink is one way in which our model provides a conservative minimum estimate for atmospheric oxygen levels.

Returning to the sediment model, we now estimate the amount of oxygen required to yield the differences in carbon preservation between the green-gray and black shales of unit 1, which we assume, from the discussion above (Sect.4.2), to be a factor of 10. Our model is constrained from modern observations through a multi-step process. Our first step is to revisit the observation that TOC preservation in modern marine sediments scales with both sedimentation rate and with sedimentary environment (Figure 3a). To proceed, therefore, we must first estimate

Biogeosciences Discuss., doi:10.5194/bg-2016-413, 2016
Manuscript under review for journal Biogeosciences
Published: 20 October 2016

the sedimentation rate for Xiamaling unit 1. From precise zircon dating, we previously determined an average linear (after compaction and lithification) sedimentation rate of 6.7 $x10^{-4}$ cm y^{-1} for a 52 meter section encompassing upper unit 3 into lower unit 2 of the Xiamaling Formation (Zhang et al., 2015). This linear sedimentation rate translates into a mass accumulation rate of 1.7 x 10^{-3} g cm^{-2} y^{-1}, assuming an average rock density of 2.5 g cm^{-3}. We call this the XML rate. We cannot be certain that this rate applies to unit 1, but to accommodate this uncertainty, we will also consider sedimentation rates of one half of the XML rate and 10 times this rate.

To demonstrate our approach, we begin with a sedimentation rate consistent with the XML rate (1.7 x 10^{-3} g cm^{-2} y^{-1}). In modern anoxic environments, sediments at this sedimentation rate experience carbon preservation of between about 20% and 30% as seen by extrapolating between existing data points in Figure 3a. This degree of carbon preservation would, therefore, be relevant for the black shales of unit 1 of the Xiamaling Formation. With a factor of 10 times lower organic carbon preservation for the green-gray shales, the carbon preservation ranges between 2% and 3% (see also Figure 3a). Similar calculations for 10 times and one half of the XML sedimentation rate are shown in Table 1. Our calculated organic carbon preservation percentages for the green-gray shales compare reasonably well with observations from modern sediments (Figure 3a).

Table 1. Carbon preservation at various rates of sediment deposition

scenario	Sed rate	%C pres	%C pres	O_2 exposure time
	g $cm^{-2}y^{-1}$	black shale	gray shale	y
XML*0.5	$0.8x10^{-3}$	12	1.2	700-6000
XML	$1.7x10^{-3}$	20-30	2-3	400-5000
XML*10	$1.7x10^{-2}$	40-80	4-8	150-2000
XML (factor 5)	$1.7x10^{-3}$	20-30	4-6	200-2000

From here, we determine the amount of oxygen exposure that sediments require to achieve the degrees of carbon preservation we have determined. The concept of oxygen exposure

Biogeosciences Discuss., doi:10.5194/bg-2016-413, 2016
Manuscript under review for journal Biogeosciences
Published: 20 October 2016

time, and its influence on carbon preservation, was initially introduced by (Hartnett et al., 1998). The idea is that more extensive organic carbon oxidation accompanies longer exposure to oxygen. As mentioned above, this idea is consistent with the experimental observations of enhanced organic matter mineralization in the presence of oxygen (Kristensen and Holmer, 2001) and the observation that carbon preservation in oxygenated environments is lower at slower rates of sediment deposition, giving more time for oxic decomposition to occur (Figure 3a). Oxygen exposure time is calculated by dividing the sediment oxygen penetration depth (cm) by the linear sedimentation rate (cm y^{-1}). In the original publication by (Hartnett et al., 1998), calculations of oxygen exposure time were mainly based on a simple model for oxygen penetration depth assuming a linear decrease in oxygen concentration in the sediment. This is typically not the case, and oxygen will generally penetrate much deeper than a linear gradient derived from the sediment surface (e.g. (Glud, 2008)). For this reason, we have compiled our own database (Table S2), which relies on actual measurements of oxygen penetration depth and for which carbon preservation (burial efficiency) can be calculated. Our compilation includes data from many parts of the global ocean and is summarized in graph form in Figure 3b. From this graph, we determine the range in oxygen exposure times associated with the different degrees of green-gray shale carbon preservation as summarized in Table 1. The oxygen exposure time results are also shown in Table 1.

With the oxygen exposure times we have determined, we can now calculate the depth of oxygen penetration necessary to generate these exposure times. To do this, we must also know the linear sedimentation rate (cm y^{-1}) which is related to the mass sedimentation rate through the following expression:

$$\text{Linear rate (cm } y^{-1}) = \text{mass rate (g cm}^{-2}\ y^{-1})*[1/(1-\phi)*\rho\ (\text{g/cm}^3)] \qquad (2)$$

where ϕ is sediment porosity and ρ is dry sediment density. These parameters are often measured, but rarely reported and not compiled, to our knowledge, for surface muds (top few cms). In our experience, a value of 2.5 g cm^{-3} is a good approximation for the dry density of sediment particles (we also used this value above to determine mass accumulation rates for the Xiamaling), and this value is typically used. Surface sediment porosities can vary, and in our experience with surface muds, a range of 0.7 to 0.9 for the upper couple of centimeters encompasses all of our dozens of observations of a great variety of marine muds, except for organic-rich euxinic

Biogeosciences Discuss., doi:10.5194/bg-2016-413, 2016
Manuscript under review for journal Biogeosciences
Published: 20 October 2016

sediments that can have porosities of > 0.95, and sands which have porosities in the range of 0.4 to 0.5. The Xiamaling sediments of unit 1, however, are relatively fine-grained silty muds, so comparisons with sands are inappropriate. In our calculations, we explore a range of porosities from 0.7 to 0.9.

A calculation of oxygen penetration depth at different porosities and different oxygen exposure times for the XML sedimentation rate is provided in Table 2. From here, we determine how much bottom water oxygen ($[O2]_{BW}$) is required to generate the oxygen penetration depths (O_2-pen) we have calculated. Generally, oxygen penetration will depend on the concentration of bottom water oxygen, the rate of sediment oxygen uptake, and the kinetics of organic carbon mineralization including any oxygen dependency on mineralization and the distribution of organic matter quality. Numerous models have been proposed relating these parameters (e.g. (Hartnett et al., 1998; Hulth et al., 1994; Rasmussen and Jørgensen, 1992)), and we will build on the simple model proposed by (Rasmussen and Jørgensen, 1992), and shown in Eq. 3, rearranged to yield $[O_2]_{BW}$.

$$[O_2]_{BW} = O_2\text{-pen}*O_2\text{-flux}/A*\phi D_{sed} \quad (3)$$

where, in addition to the terms already named, D_{sed} ($cm^2\ y^{-1}$) is the sediment diffusion coefficient for oxygen approximated as $D*\phi^2$ (Ullman and Aller, 1982), where D is the free diffusion coefficient, which we take as 536 $cm^2\ y^{-1}$, the value for seawater at 15°C (Broecker and Peng, 1982).

Table 2. Linear sedimentation rates and oxygen penetration depths (O_2 pen) for the different mass fluxes explored in our modelling.

XML*0.5			
O_2 exposure time (y)		700	6000
Porosity (ϕ)	Sed rate	O_2 pen	O_2 pen
	cm y^{-1}	cm	cm
0.7	$1.1x10^{-3}$	0.77	7.7
0.8	$1.7x10^{-3}$	1.19	11.9
0.9	$3.4x10^{-3}$	2.38	23.8

Biogeosciences Discuss., doi:10.5194/bg-2016-413, 2016
Manuscript under review for journal Biogeosciences
Published: 20 October 2016

XML sed rate			
O_2 exposure time (y)		400	5000
Porosity (ϕ)	Sed rate	O_2 pen	O_2 pen
	cm y^{-1}	cm	cm
0.7	$2.2x10^{-3}$	0.88	11.0
0.8	$3.4x10^{-3}$	1.36	17.0
0.9	$6.8x10^{-3}$	2.72	34.0
XML *10			
O_2 exposure time (y)		150	2000
Porosity (ϕ)	Sed rate	O_2 pen	O_2 pen
	cm y^{-1}	cm	cm
0.7	$2.2x10^{-2}$	3.3	44
0.8	$3.4x10^{-2}$	5.1	68
0.9	$6.8x10^{-2}$	10.2	136
XML (factor 5)			
O_2 exposure time (y)		200	2000
Porosity (ϕ)	Sed rate	O_2 pen	O_2 pen
	cm y^{-1}	cm	cm
0.7	$2.2x10^{-3}$	0.44	4.42
0.8	$3.4x10^{-3}$	0.68	6.8
0.9	$6.8x10^{-3}$	1.36	13.6

In this equation, A is variable, and a value of A=1 is consistent with a linear oxygen
435 profile in the sediment as assumed, for example, by (e.g (Hartnett et al., 1998)). This formulation is consistent with sediment containing a source of oxygen from the overlying water and a fixed sink at the depth of oxygen penetration, but no oxygen removal in between. A value of A=2 generates an equation consistent with a constant rate of oxygen removal with depth in the sediment, but no dependency of oxygen removal rate on oxygen concentration (thus zero-order

Biogeosciences Discuss., doi:10.5194/bg-2016-413, 2016
Manuscript under review for journal Biogeosciences
Published: 20 October 2016

reaction kinetics on oxygen concentration) as developed in (Rasmussen and Jørgensen, 1992). To evaluate these equations, we have compiled a database on the relationship between oxygen uptake rate and oxygen penetration depth for a broad range of marine sediments depositing in a range of different bottom water oxygen concentrations (Figure 3c; data in Table S4). We see that a value of A=2 clearly underestimates the oxygen penetration depth at a given rate of oxygen uptake (and A=1 is even worse; not shown), but the data is consistent with a value of A=4, which generates a relationship between oxygen penetration depth and oxygen uptake rate very similar to the best-fit power function of the data (O_2 uptake = $0.203O_2\text{-pen}^{-0.868}$; R^2=0.7526). With the value of A=4, Eq. 3 also seems to work through the range of oxygen concentrations explored (Figure 3c). Therefore, in subsequent modelling as described below, we will use Eq. 3 with a value of A=4 and consider it reliable for the range of oxygen concentrations explored. We note, however, that with a value of A=4, Eq. 3 is an empirical fit of the data in Figure 3c and in not based on first-principle diagenetic relationships as is true when A=1 and A=2.

Our next step is to determine rates of sediment oxygen uptake (O_2-flux) for the Xiamaling Formation green-gray shales for each of our model scenarios (Table 1), which, in modern sediments, is approximately equivalent to the total carbon mineralization rate as described in (Canfield et al., 1993). The equivalency arises because oxygen is also used to oxidize the reduced products of anaerobic mineralization. We calculate total rates of carbon mineralization by combining the burial fluxes of TOC (the product of average green-gray shale TOC concentration and the mass accumulation rate, C_{bur}) and from our estimates of carbon preservation ($\%C_{pres}$) as revealed in Table 1. Thus:

$$O_2\text{-flux} = C_{resp} = (100*C_{bur}/\%C_{pres}) - C_{bur} \quad (4)$$

The values for C_{resp} (and thus O_2-flux) obtained this way are internally consistent mass-balance values and do not require any additional assumptions. These results are shown in Table 3 for the different modeling scenarios.

Table 3. Calculations of $[O_2]_{BW}$ (μM) for our different assumptions of sedimentation rate (lowest value for each sedimentation rate in **red**).

XML*0.5			
Oxygen exposure (y)	700	6000	

Biogeosciences Discuss., doi:10.5194/bg-2016-413, 2016
Manuscript under review for journal Biogeosciences
Published: 20 October 2016

Carbon preservation (%)	1.2	1.2		
O_2-flux (mmol cm^{-2} y^{-1})	0.019	0.019		
Porosity (ϕ)	$[O_2]_{BW}$	$[O_2]_{BW}$		
	µM	µM		
0.7	**19**	160		
0.8	19	170		
0.9	27	230		
XML				
Oxygen exposure (y)	400	5000	400	5000
Carbon preservation (%)	2	2	3	3
O_2-flux (mmol cm^{-2} y^{-1})	0.029	0.029	0.015	0.015
Porosity (ϕ)	$[O_2]_{BW}$	$[O_2]_{BW}$	$[O_2]_{BW}$	$[O_2]_{BW}$
	µM	µM	µM	µM
0.7	35	440	**18**	230
0.8	36	450	19	230
0.9	51	630	26	330
XML*10				
Oxygen exposure (y)	150	2000	150	2000
Carbon preservation (%)	4	8	4	8
O_2-flux (mmol cm^{-2} y^{-1})	0.11	0.11	0.053	0.053
Porosity (ϕ)	$[O_2]_{BW}$	$[O_2]_{BW}$	$[O_2]_{BW}$	$[O_2]_{BW}$
	µM	µM	µM	µM
0.7	500	6600	**240**	3200
0.8	510	6800	250	3300
0.9	720	9600	350	4600
XML (factor 5)				
Oxygen exposure (y)	200	2000	200	2000
Carbon preservation (%)	4	4	6	6

Biogeosciences Discuss., doi:10.5194/bg-2016-413, 2016
Manuscript under review for journal Biogeosciences
Published: 20 October 2016

O_2-flux (mmol cm^{-2} y^{-1})	0.011	0.011	0.073	0.073
Porosity (ϕ)	$[O_2]_{BW}$	$[O_2]_{BW}$	$[O_2]_{BW}$	$[O_2]_{BW}$
	µM	µM	µM	µM
0.7	6.6	66	**4.4 (10.1-15.7)**[a]	44
0.8	6.8	68	4.5	45
0.9	9.6	96	6.4	64

[a]values in parenthesis after considering diffusion through the benthic boundary layer

With our calculations of O_2-pen and O_2-flux, we then use the Eq. 3 with a value of A=4, as derived above, to calculate bottom water oxygen levels at different sediment porosities. The results are shown in Table 3. Our estimates for bottom water oxygen concentration vary widely, and are highest for scenarios with the longest sediment oxygen exposure times. Long oxygen exposure times accompany deep oxygen penetration (see Table 1), and higher concentrations of bottom water oxygen are required to balance the oxygen flux into the sediment against a shallow oxygen gradient as required by the deeper oxygen penetration. In many cases, our calculations with high oxygen exposure times yield bottom water oxygen concentrations that exceed modern values by a factor of 10 or more. One could view these as upper estimates for bottom water oxygen concentrations using our modeling approach, but this is not particularly useful, as such high oxygen concentrations during Mesoproterozoic times are very unlikely.

Just as our high estimates for bottom water oxygen concentrations are unrealistically high, our minimum estimates are probably also too low. However, as our goal here is to constrain minimum oxygen levels during Xiamaling Formation deposition, we view these values as highly informative. Thus, for both the case of XML sedimentation rates and sedimentation rates one half of these (XML*0.5), a minimum estimate of 18 to 19 µM bottom water oxygen is obtained, which translates into an atmospheric oxygen concentration of 7% to 8% PAL assuming that the bottom water is in equilibrium with atmospheric oxygen at a temperature of 15°C (with an equilibrium concentration of 250 µM). As explored above, this calculation of atmospheric oxygen concentration does not account for any reduction in bottom water oxygen concentration

Biogeosciences Discuss., doi:10.5194/bg-2016-413, 2016
Manuscript under review for journal Biogeosciences
Published: 20 October 2016

that might have occurred due to water column respiration. Not accounting for this oxygen loss is another way in which our calculated atmospheric levels are minimum values.

One potential criticism of our approach is that the factor of 10 difference in carbon preservation indicated between the black shales and the green-gray shales of unit 1 is an overestimate. While the HI results, together with the TOC concentrations, strongly indicate a difference in carbon preservation between the black and green-gray shales, there is no established relationship as to how these two parameters correlate as a result of carbon mineralization. Thus, if the organic matter deposited onto the green-gray shales with a lower concentration than the black shales, then the difference in carbon preservation could be less than indicated by the difference in TOC concentration between the sediment types. We have already noted that such differences are not apparent for organic matter settling through the upper several hundred meters of oxygenated and anoxic waters of the Arabian Sea water column, but we still must entertain this possibility for the Xiamaling Formation.

Thus, we have also calculated carbon preservation, oxygen exposure times, oxygen-penetration depths and, finally, estimates for bottom water oxygen for XML sedimentation rate and a factor of 5 differences in preservation between the black and green-gray shales (Figure 3a, Tables 1-3). These results yield a lower minimum bottom water oxygen concentration of 4.4 μM and about 2 % PAL atmospheric levels. This value, however, is likely too low for two reasons. First, at both low oxygen concentrations and steep concentration gradients one must consider that oxygen is supplied to the sediment surface and into the sediment through a viscous boundary, which varies from 0.04 to 0.08 cm in continental margin sediments, where transport is by molecular diffusion (Glud, 2008). Thus, strictly speaking, our oxygen estimate of 4.4 μM (Table 3) is the oxygen concentration at the sediment surface. We calculate that a minimum $[O_2]_{BW}$ of between 10.1 μM (with a 0.04 cm boundary layer) and 15.7 μM (with a 0.08 cm boundary layer) is required to supply the 4.4 μM of oxygen needed to satisfy this minimum oxygen calculation. These $[O_2]_{BW}$ are calculated from Eq. 3 using the benthic boundary layer thickness for O_2-pen, A=1, the free diffusion coefficient for oxygen and after adding the 4.4 μM oxygen concentration at the sediment surface. The bottom water oxygen concentrations of 10.1% to 15.7μM transfer to atmospheric oxygen levels of between 4% and 6% PAL, and these should be considered the

Biogeosciences Discuss., doi:10.5194/bg-2016-413, 2016
Manuscript under review for journal Biogeosciences
Published: 20 October 2016

proper calculation values. A consideration of benthic boundary layer diffusion is not important for any of our other calculations.

Secondly, we note that low values of $[O_2]_{BW}$ in the range of even 10 μM are at odds with modern observations. Thus, when compared to anoxic settings, modern sediments depositing between the XML sedimentation rate and the XML*10 rate do not show enhanced degradation of organic matter for sediments depositing in oxygenated water with < 25 μM O_2 (Figure 3a). Indeed, this observation might suggest that our higher bottom water oxygen estimates of 18 to 19 μM are also too low. Thus, while 10 μM to 19 μM (4% to 8% PAL) is the range of minimum bottom water oxygen concentrations produced by our model, modern observations suggest that this range may be too low and that bottom water oxygen levels of >25 μM, translating to atmospheric levels of 10% PAL, are a more realistic minimum estimate.

5. Conclusions and Perspective

We combined observations of trace metal dynamics, iron speciation, and TOC and HI dynamics to determine that unit 1 of the Xiamaling Formation experienced alternating periods of deposition in oxygenated and anoxic waters. The relationship between TOC and HI indicates substantial oxic mineralization of organic matter when sediments deposited in oxygenated water. We utilized observations from modern sediment organic matter dynamics to constrain the levels of atmospheric oxygenation required to generate the differences in organic matter preservation we observed between anoxic and anoxic deposition in the Xiamaling Formation. Our modeling indicates minimum atmospheric oxygen levels at the time of Xiamaling unit 1 deposition of 4% to 8% PAL. Based on further observations from modern sediments, we believe that our estimate of 8% PAL is likely even too low.

Generally, our estimates of Mesoproterozoic atmospheric oxygen levels are consistent with the higher values of atmospheric oxygen (≥ 4% PAL) as constrained from ocean modeling (Zhang et al., 2016)while inconsistent with the lower levels of atmospheric oxygen (≤ 0.1% PAL) as constrained from chromium isotope systematics (Planavsky et al., 2014) (Cole et al., 2016a). We note, however, that the marine geochemistry of chrome, and it's isotopes, are poorly known, and we have also previously documented concerns (Zhang et al., 2016) that the samples reported in the studies, particularly (Planavsky et al., 2014), have a substantial, if not dominant, detrital

Biogeosciences Discuss., doi:10.5194/bg-2016-413, 2016
Manuscript under review for journal Biogeosciences
Published: 20 October 2016

chrome component. This would potentially compromise the interpretation of the chromium isotopes signal. In any event, observations of low atmospheric oxygen concentration during this time (<0.1% PAL) do not square with the necessity of much higher oxygen levels to drive the sedimentary carbon dynamics that we observe in the Xiamaling Formation (Zhang et al., 2016). While we do not have precise dating of unit 1 in the Xiamaling Formation, with a deposition rate from unit 2-3, the separation in time would be in the range of 20 to 25 million years. Therefore, relatively elevated levels of atmospheric oxygen appear to have been a persistent feature of the Mesoproterozoic geochemical environment for seemingly tens of millions of years. As noted previously (Zhang et al., 2016), these higher levels of atmospheric oxygen would have been sufficient to fuel animal respiration, at least at this time window in Earth history, and some 700 to 800 million years before animals first evolved.

Data Availability: All data used in this paper is provided in Table form in the supplement.

Author contributions: SZ, XW, and DEC conceived of the project, SZ, XW, HW, EUH, JS, YW, DEC did the research and SZ, XW, EUH and DEC wrote the paper.

Acknowledgments

We wish to thank Richard Boyle for discussions, Heidi Jensen and Susanne Møller for laboratory assistance and the thoughtful comments of two anonymous reviewers. We also acknowledge generous funding from the State Key Program of National Natural Science Foundation of China (41530317), the Scientific Research and Technological Development Project of China National Petroleum Corporation (CNPC 2016A-0204), and the Danish National Research Foundation (Grant DNRF53) and the ERC (Oxygen, grant 267233).

Biogeosciences Discuss., doi:10.5194/bg-2016-413, 2016
Manuscript under review for journal Biogeosciences
Published: 20 October 2016

References

Armstrong, R. A., Lee, C., Hedges, J. I., Honjo, S., and Wakeham, S. G.: A new, mechanistic model for organic carbon fluxes in the ocean based on the quantitative association of POC with ballast minerals, Deep-Sea Res Pt Ii, 49, 219-236, 2002.

Arthur, M. A. and Dean, W. E.: Organic-matter production and preservation and evolutionof anoxia in the Holocene Black sea, Paleoceanography, 13, 395-411, 1998.

Berkner, L. V. and Marshall, L. C.: On the origin and rise of oxygen concentration in the Earth's atmosphere, Journal of the Atmospheric Sciences, 22, 225-261, 1965.

Broecker, W. S. and Peng, T.-H.: Tracers in the Sea, Eldigio, Palisades, N.Y., 1982.

Brumsack, H. J.: The trace metal content of recent organic carbon-rich sediments: Implications for Cretaceous black shale formation, Palaeogeogr Palaeocl, 232, 344-361, 2006.

Butterfield, N. J.: EARLY EVOLUTION OF THE EUKARYOTA, Palaeontology, 58, 5-17, 2015.

Calvert, S. E., Pedersen, T. F., Naidu, P. D., and Vonstackelberg, U.: On the organic carbon maximum on the continental slope of the Eastern Arabian Sea J Mar Res, 53, 269-296, 1995.

Canfield, D. E.: Factors influencing organic carbon preservation in marine sediments, Chemical Geology, 114, 315-329, 1994.

Canfield, D. E.: A new model for Proterozoic ocean chemistry, Nature, 396, 450-453, 1998.

Canfield, D. E.: Sulfate reduction and oxic respiration in marine sediments: implications for organic carbon preservation in euxinic environments, Deep-Sea Research, 36, 121-138, 1989.

Canfield, D. E., Jørgensen, B. B., Fossing, H., Glud, R., Gundersen, J., Ramsing, N. B., Thamdrup, B., Hansen, J. W., Nielsen, L. P., and Hall, P. O. J.: Pathways of organic carbon oxidation in three continental margin sediments, Mar Geol, 113, 27-40, 1993.

Canfield, D. E., Raiswell, R., Westrich, J. T., Reaves, C. M., and Berner, R. A.: The use of chromium reduction in the analysis of reduced inorganic sulfur in sediments and shales, Chemical Geology, 54, 149-155, 1986.

Cole, D. B., Reinhard, C. T., Wang, X., Gueguen, B., Halverson, G. P., Gibson, T., Hodgskiss, M. S. W., McKenzie, N. R., Lyons, T. W., and Planavsky, N. J.: A shale-hosted Cr isotope record of low atmospheric oxygen during the Proterozoic, Geology, doi: 10.1130/G37787.1, 2016a. 2016a.

Cole, D. B., Reinhard, C. T., Wang, X. L., Gueguen, B., Halverson, G. P., Gibson, T., Hodgskiss, M. S. W., McKenzie, N. R., Lyons, T. W., and Planavsky, N. J.: A shale-hosted Cr isotope record of low atmospheric oxygen during the Proterozoic, Geology, 44, 555-558, 2016b.

600 Cowie, G.: The biogeochemistry of Arabian Sea surficial sediments: A review of recent studies, Prog Oceanogr, 65, 260-289, 2005.

Espitalié, J.: Use of Tmax as a maturation index for different types of organic matter: comparison with vitrinite reflectance. In: Thermal Modelling in Sedimentary Basins, Burrus, J. (Ed.), Paris, 1986.

Espitalie, J., Laporte, J. L., Madec, M., Marquis, F., Leplat, P., Paulet, J., and Boutefeu, A.: Rapid method
605 for source rocks characterization and for determination of petroleum potential and degree of evolution Rev. Inst. Fr. Pet., 32, 23-42, 1977.

Glud, R. N.: Oxygen dynamics of marine sediments, Marine Biology Research, 4, 243-289, 2008.

Hartnett, H. E., Keil, R. G., Hedges, J. I., and Devol, A. H.: Influence of oxygen exposure time on organic carbon preservation in continental margin sediments, Nature, 391, 572-574, 1998.

610 Honjo, S., Manganini, S. J., and Cole, J. J.: Sedimentation of biogenic matter in the deep ocean, Deep-Sea Research, 29, 609-625, 1982.

Hulth, S., Blackburn, T. H., and Hall, P. O. J.: Arctic sediments (Svalbard): consumption and microdistribution of oxygen, Mar Chem, 46, 293-316, 1994.

Immenhauser, A.: Estimating palaeo-water depth from the physical rock record, Earth-Sci. Rev., 96, 107-
615 139, 2009.

Keil, R. G., Neibauer, J. N., Biladeau, C., van der Elst, K., and Devol, A. H.: A multiproxy approach to understanding the "enhanced" flux of organic matter through the oxygen deficient waters of the Arabian Sea, Biogeosciences, 13, 2077-2092, 2015.

Knoll, A. H.: The multiple origins of complex multicellularity, annual review of Earth and Planetary 39,
620 217-239, 2011.

Knoll, A. H.: Paleobiological perspectives on early eukaryotic evolution, Cold Spring Harbor Perspectives in Biology, 2014. 1-14, 2014.

Kristensen, E. and Holmer, M.: Decomposition of plant materials in marine sediments exposed to different electron acceptors (O_2, NO_3^-, SO_4^{2-}), with emphasis on substrate origin, degradation kinetics,
625 and the role of bioturbation, Geochim Cosmochim Ac, 65, 419-433, 2001.

Lamborg, C. H., Buesseler, K. O., Valdes, J., Bertrand, C. H., Bidigare, R., Manganini, S., Pike, S., Steinberg, D., Trull, T., and Wilson, S.: The flux of bio- and lithogenic material associated with sinking particles in the mesopelagic "twilight zone" of the northwest and North Central Pacific Ocean, Deep-Sea Res Pt Ii, 55, 1540-1563, 2008.

630 Li, H. K., Lu, S. N., Li, H. M., Sun, L. X., Xiang, Z. Q., Geng, J. Z., and Zhou, H. Y.: Zircon and beddeleyite U-Pb dating of basic rock sills intruding Xiamaling Formation, North China, Geological Bulletin of China, 2009, 1396-1404, 2009.

Lyons, T. W. and Severmann, S.: A critical look at iron paleoredox proxies: New insights from modern euxinic marine basins, Geochim Cosmochim Ac, 70, 5698-5722, 2006.

635 Marsay, C. M., Sanders, R. J., Henson, S. A., Pabortsava, K., Achterberg, E. P., and Lampitt, R. S.: Attenuation of sinking particulate organic carbon flux through the mesopelagic ocean, Proceedings of the National Academy of Sciences of the United States of America, 112, 1089-1094, 2015.

Martin, J. H., Knauer, G. A., Karl, D. M., and Broenkow, W. W.: VERTEX: carbon cycling in the northeast Pacific, Deep-Sea Research, 34, 267-285, 1987.

640 Meng, Q. R., Wei, H. H., Qu, Y. Q., and Ma, S. X.: Stratigraphic and sedimentary records of the rift to drift evolution of the northern North China craton at the Paleo- to Mesoproterozoic transition, Gondwana Research, 20, 205-218, 2011.

Nursall, J. R.: Oxygen as a prerequisite to the origin of the metazoa, Nature, 183, 1170-1172, 1959.

Partin, C. A., Bekker, A., Planavsky, N. J., Scott, C. T., Gill, B. C., Li, B., Podkovyrov, V., Maslov, A.,

645 Konhauser, K. O., Lalonde, S. V., Love, G. D., Poulton, S. W., and Lyons, T. W.: large-scale fluctuation in precambrian atmospheric and oceanic oxygen levels from the record of U in shales, Earth Planet. Sci. Lett., 369-370, 284-293, 2013.

Planavsky, N. J., Reinhard, C. T., Wang, X. L., Thomson, D., McGoldrick, P., Rainbird, R. H., Johnson, T., Fischer, W. W., and Lyons, T. W.: Low Mid-Proterozoic atmospheric oxygen levels and the delayed

650 rise of animals, Science, 346, 635-638, 2014.

Poulton, S. W. and Canfield, D. E.: Development of a sequential extraction procedure for iron: Implications for iron partitioning in continentally-derived particulates, Chemical Geology, 214, 209-221, 2005.

Poulton, S. W. and Canfield, D. E.: Ferruginous Conditions: A Dominant Feature of the Ocean through

655 Earth's History, Elements, 7, 107-112, 2011.

Poulton, S. W., Krom, M. D., and Raiswell, R.: A revised scheme for the reactivity of iron (oxyhydr)oxide minerals towards dissolved sulfide., Geochim Cosmochim Ac, 68, 3703-3715, 2004.

Poulton, S. W. and Raiswell, R.: The low-temperature geochemical cycle of iron: from continental fluxes to marine sediment deposition, Am J Sci, 302, 774-805, 2002.

660 Pratt, L. M.: Influence of Paleoenvironmental factors on preservation of organic matter in middle cretaceous Greenhorn formation, Pueblo, Colorado, The American Association of Petroleum Geologists Bulletin, 68, 1146-1159, 1984.

Qu, Y., Pan, J., Ma, S., Lei, Z., Li, L., and Wu, G.: Geological characteristics and tectonic significance of unconformaities in Mesoproterozoic successions in the northern margin of the North China Block,
665 Geoscience Frontiers, 5, 127-138, 2014.

Raiswell, R. and Canfield, D. E.: The Iron Biogeochemical Cycle Past and Present Geochemical Perspectives, 1, 1-220, 2012.

Raiswell, R. and Canfield, D. E.: Sources of iron for pyrite formation in marine sediments, Am J Sci, 298, 219-245, 1998.

670 Rasmussen, H. and Jørgensen, B. B.: Microelectrode studies of seasonal oxygen uptake in a coastal sedment: role of molecular diffusion, Mar. Ecol.-Prog. Ser., 81, 289-303, 1992.

Riboulleau, A., Baudin, F., Deconinck, J. F., Derenne, S., Largeau, C., and Tribovillard, N.: Depositional conditions and organic matter preservation pathways in an epicontinental environment: the Upper Jurassic Kashpir Oil Shales (Volga Basin, Russia), Palaeogeogr Palaeocl, 197, 171-197, 2003.

675 Rudnick, R. L.: Composition of the continental crust. In: Treatise on Geochemistry: The Crust, Rudnick, R. L. (Ed.), Elsevier, Amsterdam, 2004.

Scott, C., Lyons, T. W., Bekker, A., Shen, Y., Poulton, S. W., Chu, X., and Anbar, A. D.: Tracing the stepwise oxygenation of the Proterozoic ocean, Nature, 452, 456-459, 2008.

Tissot, B. P. and Welte, D. H.: Petroleum formation and occurrence, Springer-Verlag, New York, 1984.

680 Ullman, W. J. and Aller, R. C.: Diffusion Coefficients in nearshore marine sediments, Limnology and oceanography, 27, 552-556, 1982.

Zhabina, N. N. and Volkov, I. I.: A method of determination of various sulfur compounds in sea sediments and rocks. In: Environmental Biogeochemistry and Geomicrobiology, Krumbein, W. E. (Ed.), Ann Arbor Science Publishers, Ann Arbor, 1978.

685 Zhang, S., Wang, X., Hammarlund, E. U., Wang, H., Costa, M. M., Bjerrum, C. J., Connelly, J. N., Zhang, B., Bian, L., and Canfie´ld, D. E.: Orbital forcing of climate 1.4 billion years ago, PNAS, 112, E1406-E1413, 2015.

Zhang, S. C., Wang, X. M., Wang, H. J., Bjerrum, C. J., Hammarlund, E. U., Costa, M. M., Connelly, J. N., Zhang, B. M., Su, J., and Canfield, D. E.: Sufficient oxygen for animal respiration 1,400 million years
690 ago, Proceedings of the National Academy of Sciences of the United States of America, 113, 1731-1736, 2016.

Biogeosciences Discuss., doi:10.5194/bg-2016-413, 2016
Manuscript under review for journal Biogeosciences
Published: 20 October 2016

Zhang, S. H., Li, Z. X., Evans, D. A. D., Wu, H. C., Li, H. Y., and Dong, J.: Pre-Rodinia supercontinent Nuna shaping up: A global synthesis with new paleomagnetic results from North China, Earth Planet. Sci. Lett., 353, 145-155, 2012.

695